SKIN INFLAMMATION

Human T cell response to CD1a and contact dermatitis allergens in botanical extracts and commercial skin care products

Sarah Nicolai[1], Marcin Wegrecki[2,3], Tan-Yun Cheng[1], Elvire A. Bourgeois[1], Rachel N. Cotton[1], Jacob A. Mayfield[1], Gwennaëlle C. Monnot[4], Jérôme Le Nours[2,3], Ildiko Van Rhijn[1], Jamie Rossjohn[2,3,5]*, D. Branch Moody[1]*, Annemieke de Jong[4]*†

During industrialization, humans have been exposed to increasing numbers of foreign chemicals. Failure of the immune system to tolerate drugs, cosmetics, and other skin products causes allergic contact dermatitis, a T cell–mediated disease with rising prevalence. Models of αβ T cell response emphasize T cell receptor (TCR) contact with peptide-MHC complexes, but this model cannot readily explain activation by most contact dermatitis allergens, which are nonpeptidic molecules. We tested whether CD1a, an abundant MHC I–like protein in human skin, mediates contact allergen recognition. Using CD1a-autoreactive human αβ T cell clones to screen clinically important allergens present in skin patch testing kits, we identified responses to balsam of Peru, a tree oil widely used in cosmetics and toothpaste. Additional purification identified benzyl benzoate and benzyl cinnamate as antigenic compounds within balsam of Peru. Screening of structurally related compounds revealed additional stimulants of CD1a-restricted T cells, including farnesol and coenzyme Q2. Certain general chemical features controlled response: small size, extreme hydrophobicity, and chemical constraint from rings and unsaturations. Unlike lipid antigens that protrude to form epitopes and contact TCRs, the small size of farnesol allows sequestration deeply within CD1a, where it displaces self-lipids and unmasks the CD1a surface. These studies identify molecular connections between CD1a and hypersensitivity to consumer products, defining a mechanism that could plausibly explain the many known T cell responses to oily substances.

INTRODUCTION

The human immune system evolved to respond to foreign microbial antigens but must also tolerate foreign compounds present in the environment, such as plants and foods. Over the past two centuries, industrialization has introduced the widespread use of chemical extraction techniques and synthetic chemistry methods. Industrial development has greatly increased the range of synthetic or purified botanical compounds to which humans are commonly exposed through pollution or the intentional use of drugs, fragrances, cosmetics, and other consumer products, especially those applied at high concentrations directly on the skin. Accordingly, the incidence of contact dermatitis has risen, especially in industrialized countries (*1*). Lifetime incidence currently exceeds 50%, making contact dermatitis the most common occupational skin disease (*2*). The essential pathophysiological feature of contact dermatitis is the allergen-specific nature of immune hypersensitivity reactions. Diagnosis relies on identifying the specific allergens to which a patient was exposed. Physicians measure local skin inflammation to a grid network of allergen patches applied to the skin as a diagnostic test. The mainstay of treatment is avoidance of exposure to named allergens.

[1]Division of Rheumatology, Immunology and Allergy, Brigham and Women's Hospital, Harvard Medical School, Boston, MA 02115, USA. [2]Infection and Immunity Program and Department of Biochemistry and Molecular Biology, Biomedicine Discovery Institute, Monash University, Clayton, Victoria 3800, Australia. [3]Australian Research Council Centre of Excellence in Advanced Molecular Imaging, Monash University, Clayton, Victoria 3800, Australia. [4]Columbia University Vagelos College of Physicians and Surgeons, Department of Dermatology, New York, NY 10032, USA. [5]Institute of Infection and Immunity, Cardiff University, School of Medicine, Heath Park, Cardiff CF14 4XN, UK.
*These authors contributed equally to this work.
†Corresponding author. Email: ad2952@cumc.columbia.edu

Considerable evidence documents a role for αβ T cells in contact dermatitis, which is caused by delayed-type hypersensitivity reactions. Gell and Coombs (*3*) defined type IV reactions as "delayed-type" hypersensitivity because they appear after 72 hours. Type IV reactions are T cell mediated and are worsened after repeated exposure to allergens. During the sensitization phase, naive T cells are activated in a process that involves Langerhans cells and dermal dendritic cells (*2*). In the elicitation phase, T cells cause inflammatory manifestations in the skin. Biologists' views of T cell response are strongly influenced by the known mechanisms by which T cell receptors (TCRs) recognize peptide antigens bound to major histocompatibility complex I (MHC I) and MHC II proteins (*4*–*6*). Yet, most known contact allergens are nonpeptidic small molecules, cations, or metals that are typically delivered to skin as drugs, oils, cosmetics, skin creams, or fragrances (*1*, *2*). Thus, the chemical nature of contact allergens does not match the chemical structures of most antigens commonly recognized within the TCR-peptide–MHC axis.

This apparent disconnect, which represents a core question regarding the origin of delayed-type hypersensitivity, might be explained if MHC proteins use atypical binding interactions to display nonpeptidic antigens to TCRs. For example, the antiretroviral drug abacavir binds within the human leucocyte antigen (HLA)–B*57:01 groove to alter the seating of self-peptides, creating neo-self epitopes (*7*). Similarly, the MHC class II protein encoded by HLA-DP2 can bind beryllium, thereby plausibly altering the MHC-peptide complex shape to enable binding of an autoreactive TCR (*8*). Here, autoimmune response to nonpeptidic compounds still involves peptides in some way and is linked to a specific HLA allomorph that uses a defined structural mechanism. A second general model is that nonpeptidic allergens form covalent bonds with peptides in vivo. Such "haptenation"

reactions might create hybrid molecules with peptide-based MHC binding moieties and TCR epitopes formed from the haptenizing drug or chemical. This concept derived from Landsteiner's landmark studies with 2,4-dinitrophenols (*9*) and evolved into broader predictions that drugs could haptenate peptides or innate receptors (*10*). Some evidence indicates that drugs can generate immune hypersensitivity reactions via haptenation. For example, sulfamethoxazole, lidocaine, penicillins, lamotrigine, carbamazepine, *p*-phenylenediamine, or gadolinium can bind peptides, MHC proteins, or TCRs (*11*–*16*). Although the haptenation hypothesis is broadly taught to physicians, the extent to which it accounts for the larger spectrum of contact allergens remains unknown (*17*).

Both of these models derive from the premise that αβ T cell responses are mediated by MHC-encoded proteins and emphasize atypical modes of peptide presentation. Putting aside this premise, we tested a straightforward model whereby drugs and other nonpeptidic contact allergens are presented by a system that evolved to present nonpeptidic antigens to T cells (*18*). CD1 proteins are MHC I–like molecules that fold to form an antigen binding cleft composed of two pockets, A′ and F′, which are larger and more hydrophobic than the clefts present in MHC I and MHC II proteins (*19*, *20*). Most published studies of human CD1 proteins (CD1a, CD1b, CD1c, and CD1d) emphasize display of amphipathic membrane phospholipids and sphingolipids. The alkyl chains bind within and fill up the cleft of CD1, and the polar head groups, composed of carbohydrates or phosphate esters, protrude through a small portal (F′ portal) to lie on the outer surface of CD1, where they are presented to TCRs (*21*).

Whereas most known CD1-presented antigens are amphipathic lipids, some evidence suggests that CD1 proteins mediate recognition of nonlipidic, drug-like molecules. For example, CD1d mediates T cell response to phenyl pentamethyldihydrobenzofuran sulfonates (PPBFs) (*22*), and chemically reactive small molecules can influence CD1-restricted T cell response by an unknown mechanism that might involve induced lipid autoantigen synthesis (*23*). PPBFs lack aliphatic hydrocarbon chains that define lipids, and they are instead ringed, sulfated small molecules that chemically resemble allergenic drugs, such as sulfonamide antibiotics and furosemide. However, PPBF antigens are much smaller than the known volume of CD1d cleft. Unlike amphipathic lipids, they lack a defined lipid anchor and hydrophilic head group (*22*), raising questions about how PPBFs could bind within CD1d and yet protrude in some way for TCR contact.

Among human CD1 isoforms, we focused on CD1a because it is abundantly expressed on epidermal Langerhans cells and dermal dendritic cells, which are implicated in contact dermatitis (*24*). In addition, CD1a-autoreactive T cells home to the skin, and polyclonal autoreactive T cells derived from blood and skin show higher responses to CD1a as compared with other CD1 proteins (*25*, *26*). In addition, surface CD1a proteins can rapidly capture extracellular antigens using mechanisms that do not require complex mechanisms of antigen processing within the endosomal network (*27*, *28*). Recently, transfer of the human CD1a gene into mice (*29*) was found to augment intradermal T cell responses to the natural, plant-derived compound, urushiol (*30*). Actual CD1a-mediated T cell responses to commonly used drugs or contact allergens in consumer goods are, to our knowledge, unknown.

As a screen for the most common and clinically important contact dermatitis antigens, we tested for human T cell response to compounds embedded in the thin-layer rapid use epicutaneous (T.R.U.E.) test (or Truetest), which is broadly used in dermatology and allergy clinics to screen patients for contact dermatitis allergens that are most commonly encountered in medical practice. This approach identified a human T cell response to a tree oil–derived contact allergen known as balsam of Peru. Larger-scale screens defined the general chemical requirements for a T cell response to oily substances and discovered additional contact allergens presented by CD1a, including farnesol. The crystal structure of the CD1a-farnesol complex and study of the self-lipids bound to CD1a provided evidence for a molecular mechanism for recognition of a contact allergen, explaining how small antigens sequestered fully within CD1a can lead to T cell responses through the absence of interference with CD1a-TCR contact.

RESULTS

Balsam of Peru binds CD1a and activates T cells

To determine whether CD1a can present contact allergens to T cells, we initially used the CD1a-restricted αβ T cell line known as BC2 for testing response to the T.R.U.E. test panel 1 (Truetest 1) (fig. S1). BC2 is a T cell line derived from peripheral blood T cells of a blood bank donor and has previously been shown to be activated by CD1a loaded with small hydrophobic self-lipids (*31*). Normally, the Truetest panel consists of compounds arrayed on sterile matrix, which is placed on patient skin. Localized erythema occurring in vivo on skin 2 to 5 days after exposure is considered a positive test, allowing allergen identification based on position in the grid. For testing in vitro, individual allergen patches and untreated patch matrix (control patch) were cut apart with sterile technique. Patches were soaked in media and removed (soaking method) or inserted into wells to contact (contact method) CD1a-transfected K562 (K562-CD1a) antigen-presenting cells (APCs). We saw a modest response to K562-CD1a in the absence of added patch material using interferon-γ (IFN-γ) enzyme-linked immunosorbent assay (ELISA), as expected on the basis of the known CD1a autoreactivity of the BC2 T cell line (fig. S1A).

Compared with the control patch, most of the antigen-containing patches, including nickel, potassium dichromate, colophony, lanolin, and paraben, showed no effect. A combination of molecules known as "fragrance mix 1" showed slight suppression of cytokine release, consistent with toxicity to cells (fig. S1A). Cobalt, neomycin, and ethylenediamine dihydrochloride showed small increases in IFN-γ at some doses tested but not reproducibly in subsequent assays. In contrast, balsam of Peru showed a significant response above background (fig. S1A), which also repeated in subsequent assays (fig. S1B and Fig. 1A). Response to balsam of Peru was not seen with patch soaking (fig. S1B), indicating that the stimulatory factor(s) was not physically released from the patch. Overall, the screen suggested a T cell response to balsam of Peru embedded in Truetest patches, leading to focused studies of this natural botanical extract.

Balsam of Peru is a resin from the South American tree *Myroxylon balsamum*, which has a vanilla scent and is used as a fragrance and flavor in many personal care products such as skin creams and toothpaste. Balsam of Peru is a common contact allergen seen in medical practice, where it causes severe skin rash in allergic individuals (*32*, *33*). We tested balsam of Peru extract and oily substances derived therefrom, which is known as balsam of Peru oil. Both preparations are commonly used in consumer products. BC2 T cells were activated

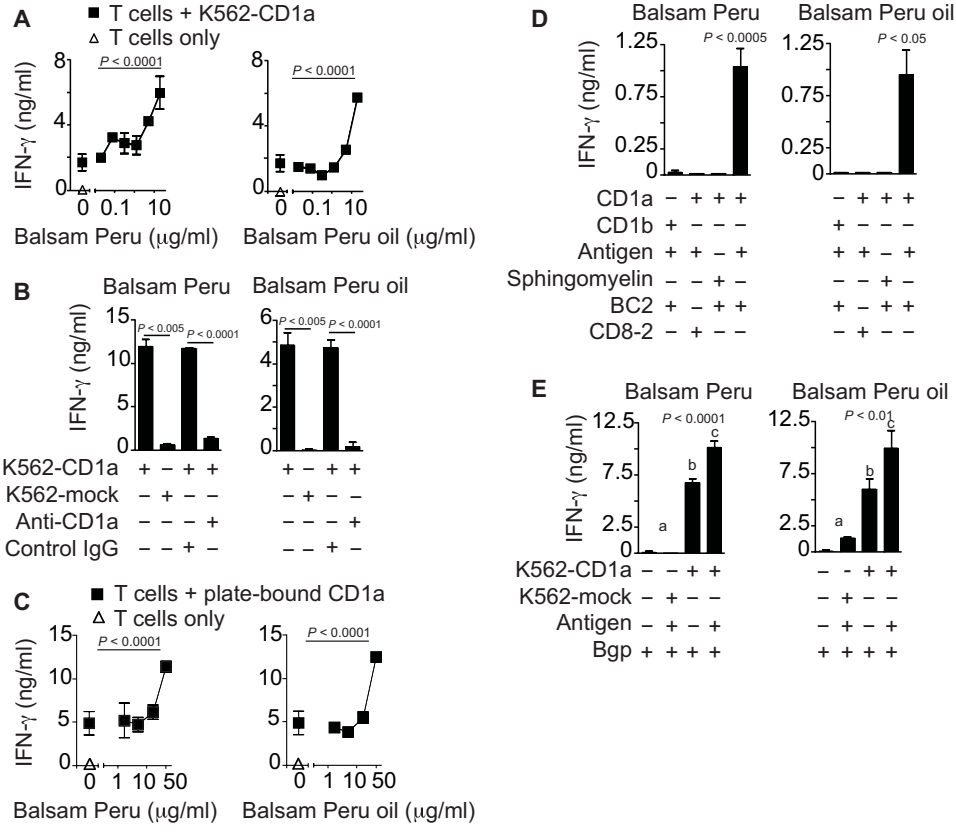

Fig. 1. Balsam of Peru activates T cells via a CD1a-dependent, APC-independent mechanism. (**A** to **E**) T cell lines with CD1a autoreactivity (BC2 and Bgp) or foreign antigen reactivity (CD8-2) were tested for activation to lipids using IFN-γ ELISA in cellular assays with CD1a-transfected K562 cells (K562-CD1a) or mock-transfected K562 cells (K562-mock) (A, B, and E) or on streptavidin plates coated with biotinylated CD1 proteins (C and D). Data are representative of three or more experiments each with the mean of triplicate measurements shown with SD. The significance of lipid concentration on IFN-γ release was tested by one-way ANOVA (A and C). Relevant pairwise comparisons were tested using Welch's *t* test (B). Post hoc comparison of marginal means after adjustment by the Sidak method was used to group treatments at the specified significance level after a significant result by two-way ANOVA (D). Post hoc comparison by least squares means after adjustment by the Sidak method was used to group treatments with nonoverlapping marginal means and 95% confidence levels into a, b, or c at the specified significance level after a significant result by two-way ANOVA (E). IgG, immunoglobulin G.

by both preparations, establishing a T cell dose response to a common botanical extract used in consumer goods (Fig. 1A).

Given the unusual chemical nature of oily substances found in Balsam of Peru oil, we considered candidate mechanisms of T cell activation other than antigen display by CD1a. In theory, compounds might undergo peptide haptenation reactions for presentation by MHC proteins, but this possibility was less favored because K562 cells express very low or undetectable MHC I and MHC II (*25*). Oily mixtures might influence cellular lipid production (*23*) or contain mitogens that cross-link CD3 complexes or broadly activate lymphocytes via TCR-independent mechanisms (*34*). To determine the cellular and molecular mechanisms of T cell stimulation, we measured T cell activation by K562 APCs and by biotinylated CD1a proteins bound to avidin-coated plates. As assessed with anti-CD1a blocking antibodies and K562 cells lacking CD1a, CD1a was required for the BC2 response to crude balsam of Peru and oils derived therefrom (Fig. 1, B and C). Treating plate-bound CD1a protein with balsam of Peru was sufficient to activate the BC2 response, albeit at higher doses than with antigen in the presence of CD1a-expressing cells (Fig. 1C). Thus, APCs facilitate some aspects of T cell response, but clear activation in APC-free systems ruled out that antigen processing is required. As a specificity control, BC2 did not respond to a structurally unrelated lipid, sphingomyelin, which is a known ligand for CD1a (Fig. 1D) (*35*). These results were most consistent with CD1a forming complexes with some molecule in these antigen preparations. Further specificity controls showed that balsam of Peru preparations did not activate a CD1a-restricted T cell clone, CD8-2, that recognizes CD1a presenting a mycobacterial antigen (Fig. 1D) (*18*, *36*). This finding, along with the absolute requirement for CD1a in all recognition events, strongly indicated that these substances are not mitogens. However, both balsam of Peru and balsam of Peru oil did activate another CD1a-autoreactive T cell line, Bgp (*31*). This indicates that balsam of Peru response was not limited to the BC2 T cell line (Fig. 1E).

Chemical composition of balsam of Peru

Next, we sought to pinpoint chemical structures of the antigenic substances. Balsam of Peru is a complex botanical extract, with the most abundant components previously reported to be benzyl cinnamate and benzyl benzoate (*37*). Silica thin-layer chromatography (TLC) showed that crude balsam of Peru contained hydrophilic compounds that remained near the origin, as well as two dark spots that comigrate with synthetic benzyl benzoate and benzyl cinnamate standards (Fig. 2A). As expected, oils extracted from balsam of Peru lacked the hydrophilic compounds that adhered at the origin. Balsam of Peru oil generated one dark spot that comigrated with benzyl benzoate. More sensitive methods of positive-mode nanoelectrospray ionization mass spectrometry (MS) (Fig. 2B) detected sodium adducts $[M+Na]^+$ of benzyl cinnamate [mass/charge ratio (*m/z*) 261.3] and benzyl benzoate (*m/z* 235.3) in both preparations. The signal for benzyl benzoate was ~10-fold stronger than for benzyl cinnamate in balsam of Peru oil. Thus, benzyl cinnamate was present in both preparations, but its concentration was below the threshold of detection by TLC.

Benzyl cinnamate and benzyl benzoate are CD1a-presented antigens

False-positive results from trace contaminants in natural preparations occur, so we tested whether benzyl benzoate and benzyl cinnamate, provided as purified synthetic molecules, activated CD1a-restricted T cells. We observed T cell activation in response to both synthetic

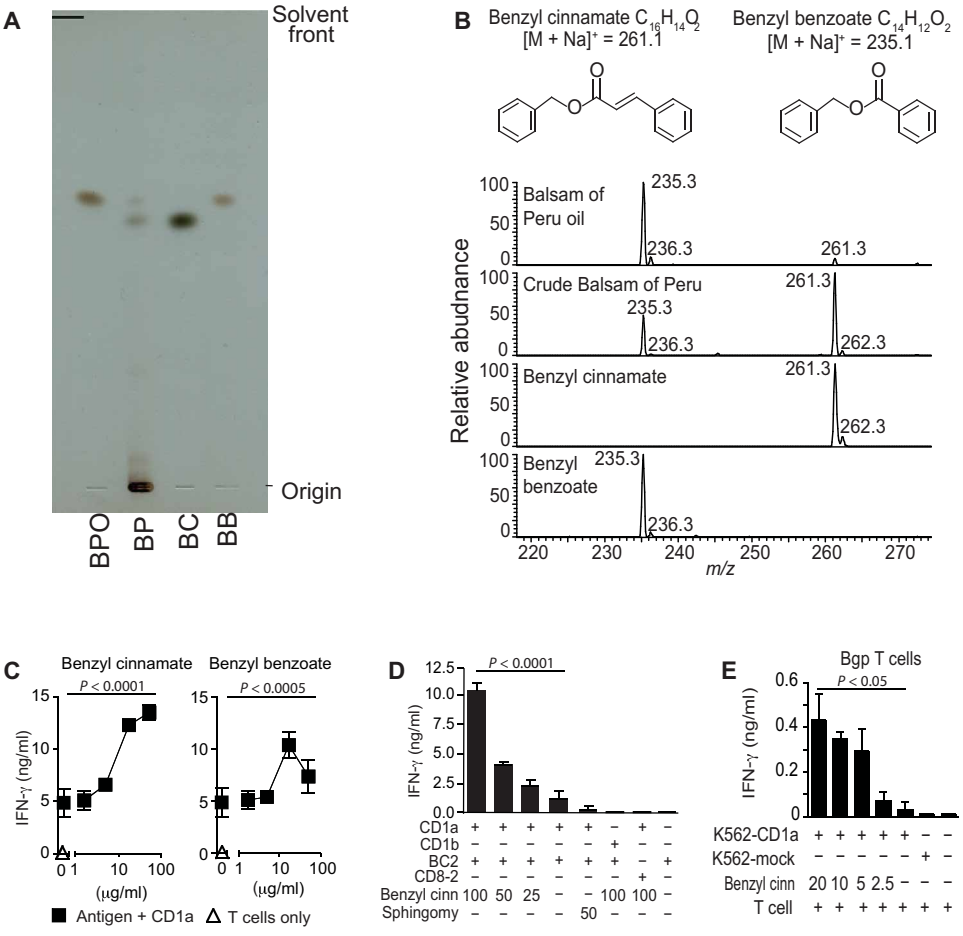

Fig. 2. Chemical analysis of antigenic substances in balsam of Peru. (**A**) Normal-phase silica TLC plate resolves balsam of Peru oil (BPO), crude balsam of Peru (BP), synthetic benzyl cinnamate (BC), and synthetic benzyl benzoate (BB). (**B**) Structures of benzyl cinnamate and benzyl benzoate are shown with the expected mass of sodium adducts $[M+Na]^+$, which were detected in positive-mode nanoelectrospray ionization MS. (**C** to **E**) T cell clones that are autoreactive to CD1a (BC2) or foreign antigen (CD8-2) were tested for response to antigens (μg/ml) or SM (sphingomy) by IFN-γ ELISA in cellular (E) or CD1a-coated plate (C and D) assays. Data are representative of three or more experiments, each shown as the mean of triplicate samples ± SD. The significance of lipid concentration on IFN-γ release was tested by one-way ANOVA (C). The significance of benzyl cinnamate and benzyl benzoate concentration on IFN-γ release and of the effects of CD1b or CD8-2 T cells were tested by two-way ANOVA (D and E).

molecules, and the response was dependent on precoating the plate with CD1a. We observed a stronger and more potent response to benzyl cinnamate (Fig. 2C), which was then used for further mechanistic studies. Detailed testing of BC2 and CD8-2 activation by benzyl cinnamate confirmed the dose dependence, CD1a dependence, and TCR specificity of the T cell response to benzyl cinnamate (Fig. 2D). Sphingomyelin, a known CD1a ligand (*31*), which has a bulky polar head group, did not activate T cells. Responses to benzyl cinnamate were seen in two T cell lines, BC2 and Bgp (*31*). Benzyl cinnamate and benzyl benzoate were efficiently presented by plate-bound CD1a proteins after a short coincubation, demonstrating the lack of a cellular processing requirement (Fig. 2, C and D). These findings are most consistent with the formation of CD1a–benzyl cinnamate complexes as the target of T cell response. Thus, tree oils that are known to act as potent contact hypersensitivity agents also function as T cell stimulants that act via CD1a.

Shared structures and size among oily antigens

The dual benzyl rings present in benzyl cinnamate and benzyl benzoate (Fig. 2B) are chemically different from the alkyl chains present in most CD1-presented antigens. However, they are notably similar to the dually ringed structure present in the unusual nonlipidic antigen presented by CD1d known as PPBF (*22*). All three nonlipidic T cell stimulants are smaller (212 to 345 Da) than most previously known CD1-presented lipid antigens (~700 to 1500 Da) (*21*). Prior CD1-lipid structures (*21*) established a widely accepted mechanism whereby the acyl chains rest inside the hydrophobic clefts of CD1 proteins, so that hydrophilic head groups protrude outside CD1 and form epitopes that specifically contact TCRs (Fig. 3A) (*38*). In contrast, the antigenic tree oils identified here lack any identifiable polar group that could function as a TCR epitope (Fig. 3B). Further, the size of the carbon skeletons of benzyl benzoate and benzyl cinnamate (C14 to C16) are substantially smaller than other CD1 antigens (C20 to C40) and the estimated capacity of the CD1a cleft (~C36) (*19*, *39*, *40*). Because tree oils are apparently too small to fill the CD1a cleft we hypothesized that they might not form TCR epitopes and so function outside the main CD1 antigen display paradigm. For example, interactions within the CD1a cleft might alter the shape of CD1-lipid complexes from the inside (*41*). Alternatively, similar to recent studies of CD1a (*31*, *35*) and CD1c (*42*), tree oils might displace endogenous lipids, whose large head groups interfere with TCR contact with CD1a. This emerging model is known as the "absence of interference" because carried lipids do not contact TCRs directly but instead bind CD1 in a manner that allows direct contact between CD1 and the TCR (*31*, *35*).

Testing rings, unsaturations, and molecular size

The approach to testing chemical features was guided by the observation that squalene, benzyl benzoate, and benzyl cinnamate have ringed or unsaturated structures that chemically constrain molecules, rendering them bulky and rigid. Using tree oils and skin oils as lead compounds (Fig. 3B) to generate a larger test panel (Fig. 3, C to E, and fig. S2), we surveyed 29 structurally related molecules that differed in size, saturation, branching patterns, or ringed structures. Fifteen compounds, including examples among branched (Fig. 3C), ringed (Fig. 3, D and E), and saturated or unsaturated fatty acyl compounds (fig. S2), were recognized. This moderately promiscuous pattern was markedly different from T cell responses to glycolipids

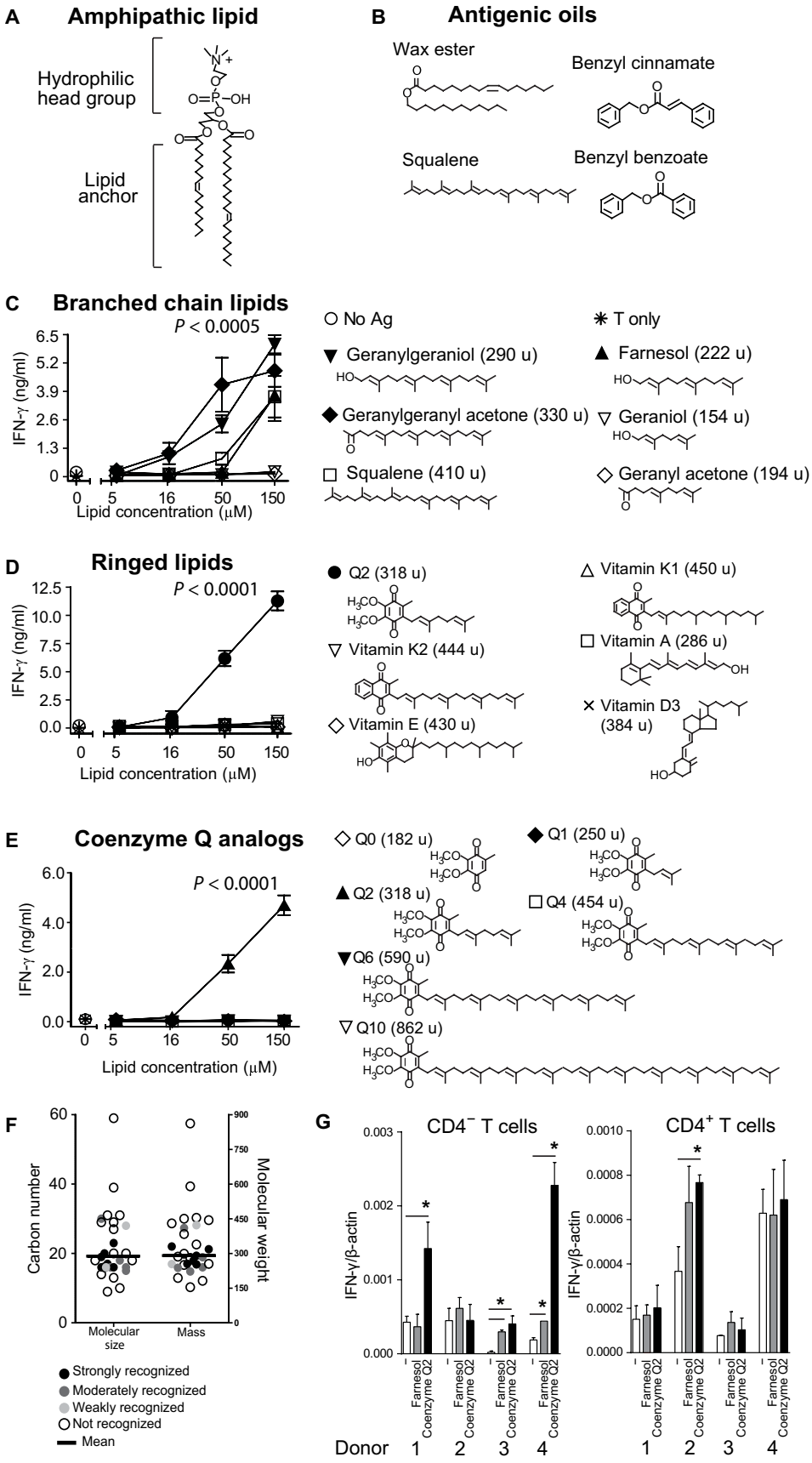

Fig. 3. T cell responses to chemically diverse oily substances. (**A**) Using PC as an example, CD1 ligands are often composed of head groups and lipid anchors, but (**B**) recently identified CD1a presented antigens are oils. (**C**) BC2 T cells were tested for cytokine release in response to small hydrophobic molecules pulsed on plate-bound CD1a pretreated with acidic citrate buffer to strip ligands (*31*). Tested compounds are classified into groups based on the presence of branched-chain unsaturated lipids structurally related to squalene, (**D**) ringed lipids structurally related to benzyl cinnamate, or (**E**) molecules that show branched, polyunsaturated, and ringed structures, such as coenzyme Q2. Results of triplicate analyses are shown as means ± SD with each compound tested two or more times. Post hoc comparison by marginal means of the interaction term between lipid and concentration after adjustment by the Sidak method was used to group treatments by nonoverlapping 95% confidence levels at the specified significance level after a significant result by two-way ANOVA. (**F**) The size of all tested antigens is shown on the basis of the number of carbon atoms (C) or mass [atomic mass units (u)], as compared with the volume of the CD1a cleft, which has been measured at 1650 Å^3, and can accommodate ~36 methylene units (C36) (*19*, *40*). (**G**) Purified T cells (CD4$^-$ and CD4$^+$) were incubated overnight with plate-bound CD1a, either mock treated or pretreated with the indicated antigens (50 μg/ml). Real-time PCR of IFN-γ mRNA relative to β-actin.*$P < 0.05$, two-sided Student's *t* test, antigen-treated compared with mock-treated CD1a.

such as α-galactosyl ceramide or glucose monomycolate, where altering a single stereocenter on the carbohydrate epitope abolished recognition (*43*, *44*). However, not every oily substance was sufficient to activate T cells.

Considering the particular chemical structures that control response, squalene is a C30 polyunsaturated branched-chain lipid antigen (Fig. 3B) (*31*). We found cross-reactivity to structurally related C20 geranylgeraniol and C23 geranylgeranylactone, as well as C15 farnesol, but not smaller geraniol-based compounds (Fig. 3C). The farnesol response is notable because it is also a contact allergen in Truetest panel 2 (*45*) (Fig. 1) and so represents another link between contact allergens and CD1a antigens. Further, considering molecules with branched and ringed structures related to benzyl cinnamate, we identified a new antigen, coenzyme Q2 (Fig. 3D). Although coenzyme Q2 has not been described as a contact allergen, idebenone, which has an identical head group (2,3-dimethoxy, 5-methyl, 1,4-benzoquinone) but a less hydrophobic lipid tail, composed of a 10-carbon alkyl chain with a hydroxyl

group, is a well-known skin allergen (*46*–*48*). In addition, in our CD1a plate assays, idebenone stimulated a dose-dependent T cell response, supporting a link between coenzyme Q2–related structures and contact allergens (fig. S3). Vitamin E, a known skin allergen, did not induce a response in this BC2-based screening. However, this does not exclude the existence of CD1a-restricted T cells to this hydrophobic compound within a polyclonal T cell repertoire.

The identification of a strong stimulatory response to coenzyme Q2 prompted screening of coenzyme Q length analogs, finding optimal response to coenzyme Q2 but not larger or smaller chain length analogs (Fig. 3, D and E). Last, comparison of 12 fatty acyl analogs consistently showed stronger response when the normally charged carboxylate group was capped by a methyl, alkyl, or other structure to generate a nonpolar molecule (fig. S2). A weak effect was seen in some cases, where potency was increased by cis unsaturation.

In summary, compared with highly flexible lipids with saturated alkyl chains, an unsaturated, ringed, or branched structure correlated with higher response. However, very highly constrained or bulky structures, such as vitamin A, vitamin D, and vitamin E, were not recognized. Considering molecular size, response was optimal with compounds (222 to 410 Da, C15 to C30) that were near the middle of the size range tested (154 to 862 Da, C9 to C59) (Fig. 3F). These optima were considerably smaller than known CD1 antigens (~700 to 1500 Da). Even the largest stimulatory compound, squalene (C30, 410 Da), was substantially smaller than the predicted number of methylene units (~C36) that would fill the CD1a cleft (1650 $Å^3$) (*19*, *40*). Unlike molecules that form antigenic epitopes for TCRs, no single molecular variant could be assigned as essential for T cell activation.

Last, to determine whether the identified link between CD1a and contact allergens is generalizable to polyclonal T cells and among genetically unrelated human donors, we screened purified polyclonal T cells ($CD4^+$ and $CD4^-$) from blood bank donors and determined their response to plate-bound CD1a preloaded with either farnesol or coenzyme Q2. As also seen in clinical evaluation of contact dermatitis patients, not all patients responded to every antigen, but we observed polyclonal responses to both antigens in two or more subjects using sensitive real-time quantitative polymerase chain reaction (qPCR) testing of IFN-γ response (Fig. 3G). Responses were seen in the $CD4^+$ T cell fractions but were stronger in the $CD4^-$ T cell fraction (Fig. 3G). This suggests that the normal T cell repertoire contains T cells that respond to CD1a–contact allergen complexes. Similarly, in a different set of donors, T cell responses were detected to benzyl cinnamate–loaded CD1a (fig. S4). Together, these results support the broader relevance of these CD1a allergens beyond the specificity of two T cell lines.

CD1a-lipid binding to the TCR

Farnesol is a common additive to cosmetics and skin creams, where its use requires precaution labeling, based on its recognized role as a contact allergen (*45*). Farnesol testing is routine in clinical practice, where it is present in the "fragrance mix 2" in Truetest patches. Farnesol can also be tested as a pure compound, generating responses in ~1% of people with suspected contact dermatitis (*45*). After the screen identified a farnesol response (Fig. 3C), we observed reproducible and dose-dependent response for BC2 in the CD1a-coated plate assay (Fig. 4A). Thus, farnesol was unlikely to be modified before recognition and was likely recognized by the BC2 TCR as a CD1a-farnesol complex.

To test this hypothesis, we loaded farnesol onto biotinylated CD1a monomers, generated fluorescent tetramers, and stained the BC2 T cell line and a control line. In several attempts with differing protocols, we failed to detect staining with CD1a-farnesol tetramers above background levels seen with farnesol-treated CD1b tetramers (fig. S5). Turning to surface plasmon resonance (SPR), we produced the BC2 TCR heterodimer in vitro and measured its binding to untreated CD1a carrying mixed endogenous lipids (CD1a-endo), CD1a that was treated with media (CD1a-mock), and CD1a treated with farnesol (CD1a-farnesol) after coupling to SPR chips. The BC2 TCR bound to all three complexes with low but measurable binding affinities for CD1a-endo [dissociation constant (K_D) = 123 μM], CD1a-mock (K_D = 144 μM), and CD1a-farnesol (K_D = 123 μM) (Fig. 4B). SPR is known to be more sensitive than tetramer staining (*49*), so the relatively low affinity interactions likely explained the absent tetramer staining. Yet, interactions are still in the physiological range, demonstrating direct binding between the BC2 TCR and CD1a. However, the cross-reactivity of the BC2 TCR to three forms of CD1a left unclear the role of farnesol or other carried lipids in mediating CD1a-TCR interactions.

Lipid analysis of CD1a-lipid complexes

A recently proposed but unproven hypothesis is small hydrophobic lipids could fully sequester within CD1a (*31*, *50*), displacing larger endogenous self-lipids that cover TCR epitopes on the outer surface of CD1a. Therefore, we undertook direct biochemical analysis of CD1a-lipid complexes formed in vitro with detergents and stimulatory substances, analyzing elutable lipids using high-performance liquid chromatography–mass spectrometry (HPLC-MS). First, we addressed the trivial possibility that the lack of effect of farnesol treatment on TCR binding to CD1a resulted from the lack of farnesol loading onto CD1a. Analysis of eluents from farnesol-treated CD1a monomers was initially inconclusive because farnesol is a nonpolar alcohol and does not readily adduct the cations or anions needed for MS detection. However, building on the fortuitous detection of a positively charged dehydration fragment $[M\text{-}H_2O + H]^+$ generated in the MS source (*31*), we could reliably detect the equivalent product ($C15H25^+$; *m/z* 205.196) from a farnesol standard. Subsequently, we detected strong signal for this product from farnesol-treated CD1a proteins but not CD1a-endo, directly documenting farnesol in CD1a complexes (Fig. 4D).

Further, the HPLC-MS–based platform allowed broader analysis of the lipid ligands carried in CD1a-endo and CD1a-farnesol complexes. Similar to prior reports (*31*, *35*), we could detect many ions in CD1a-endo eluents, which were self-lipids captured during protein expression in cells. Focusing on specific classes of lipids, including neutral lipids, phospholipids, and sphingolipids, we could identify many self-ligands. CD1a-endo complexes carried at least three molecular species of diacylglycerol (DAG), six phosphatidylcholine (PC), six sphingomyelin (SM), and two phosphatidylinositol (PI) species. Initially, these identifications were based on the expected early (DAG) or later (PI, PC, and SM) retention time, as well as match of the detected *m/z* value with the expected mass of these ligands (Fig. 4, E to F). For one lead compound in each class, we confirmed the identification using collision-induced dissociation MS, which demonstrated the characteristic phosphocholine, phosphoinositol, sphingolipid, or DAG fragments (Fig. 4G).

Elution analysis of farnesol-treated CD1a directly demonstrated farnesol loading (Fig. 4D). The comparison of CD1a-endo and

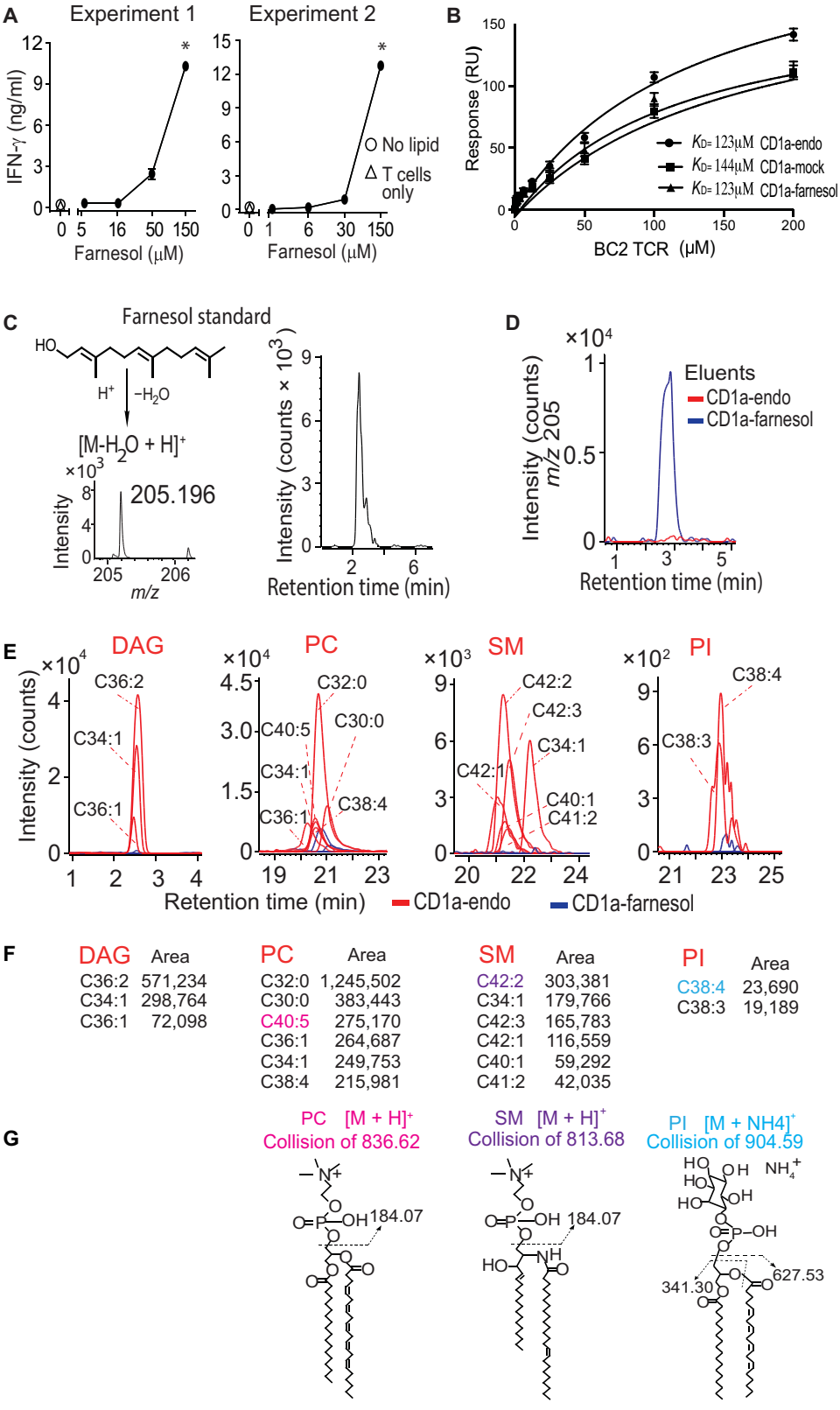

Fig. 4. CD1a-farnesol complexes. (**A**) IFN-γ release by BC2 T cells in response to CD1a-coated plates treated with farnesol was measured. Asterisk (*) indicates that the significance of lipid concentration on IFN-γ release was assessed by marginal means with adjustment by the Sidak method after a significant result by ANOVA, treating experiments 1 and 2 as blocks. At the highest concentration of farnesol in both experiments, nonoverlapping 95% confidence intervals were observed at $P < 0.001$. (**B**) Affinity measurements (K_D) by SPR in response to the recombinant BC2 TCR binding biotinylated CD1a directly isolated from cells (CD1a-endo), CD1a pretreated with farnesol (CD1a-farnesol), or CD1a treated with buffer (CD1a-mock). Positive-mode HPLC-MS analysis of a farnesol standard (**C**) and eluents from farnesol-treated CD1a (**D**) demonstrated ions that matched the expected mass (*m/z* 205.195) of an indicated dehydration product with a retention time of 2.9 min. (**E** and **F**) Lipid eluents from CD1a-endo and CD1a-farnesol were analyzed by positive normal-phase HPLC-QToF-MS. Ion chromatograms were generated at the nominal mass values of DAG, PC, SM, and PI, which are shown as CX:Y, where X is the number of methylene units in the combined lipid chains, and Y is the total number of unsaturations. (**G**) Compound identifications were based on the unknown matching of the retention time and mass of standards. Further, one compound in the PC, SM, and PI families (shown in color) underwent collision-induced dissociation MS analysis to generate the indicated diagnostic fragments. RU, resonance units.

CD1a-farnesol eluents showed complete or nearly complete suppression of ion chromatogram signals corresponding to all the 17 tested self-lipids (Fig. 4E, blue). Although the conditions used to load farnesol in vitro are not the same as those in immunological assays, these findings suggest high occupancy of CD1a proteins by farnesol and that farnesol and self-lipids are not simultaneously bound. Together, these data support a simple model for the cross-reactivity, where the TCR binds CD1a carrying either farnesol or certain self-lipids that permit recognition. Treatment of CD1a with farnesol displaces lipids with hydrophilic head groups to generate more homogeneously liganded CD1a proteins (Fig. 4, D and E).

CD1a-farnesol crystal structure overview

To determine the structural basis of farnesol response, we solved the CD1a-farnesol crystal structure at 2.2-Å resolution (table S1). The electron density for the bound farnesol and surrounding CD1a residues were unambiguous (fig. S6), allowing determination of the position and orientation of farnesol within the cleft (Fig. 5, A and B). Unlike covalent binding of vitamin B metabolites to major histocompatibility

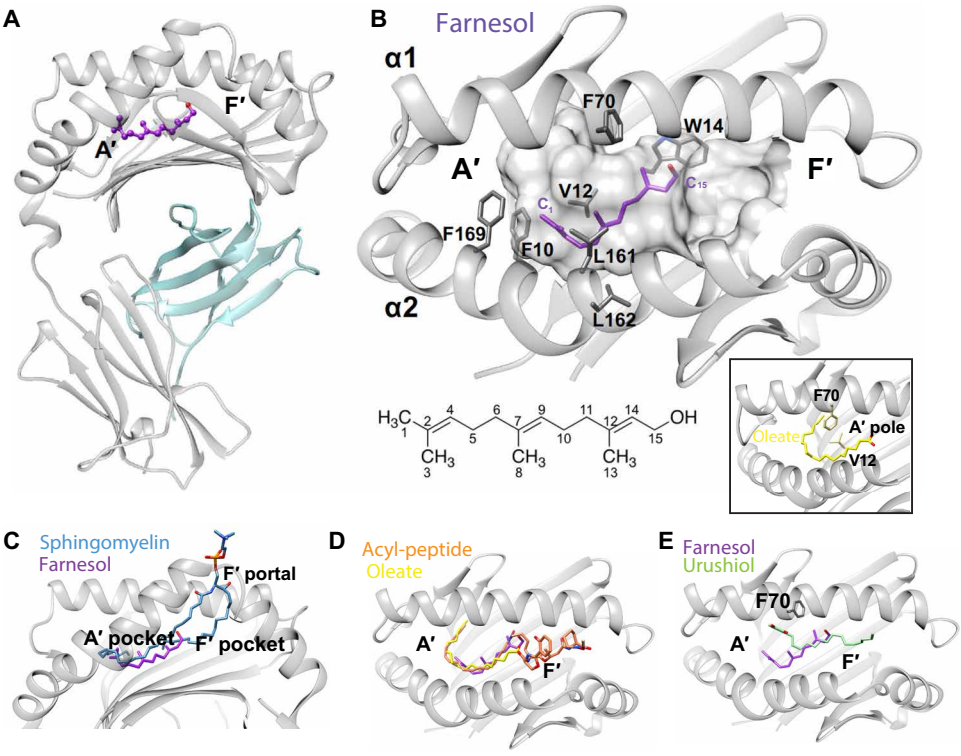

Fig. 5. Crystal structure of CD1a-farnesol complexes. (**A**) Overview of the binary crystal structure of CD1a (gray)–farnesol (purple)/β2m (cyan). (**B**) Molecular interactions of farnesol (purple) with the hydrophobic residues within CD1a binding cleft (gray surface). The side chains of the residues within a 4-Å distance from the lipid are shown. A diagram of *trans,trans*-farnesol with carbon numbering is shown. The A′ pole formed by V12-F70 interaction in the context of oleic acid–bound CD1a pocket [Protein Data Bank (PDB) ID: 4X6D] is highlighted in the inset. (**C** to **E**) Superimposition of CD1a bound to farnesol and SM [PDB ID: 4X6F (*35*)] (C), lipopeptide [PDB ID: 1XZ0 (*40*)] (D), and urushiol [PDB ID: 5J1A (*30*)] (E).

complex class I–related protein (MR1) (*51*) and the predictions of haptenation models, we find no evidence for haptenation of CD1a residues by farnesol.

Instead, the notable finding is that farnesol is deeply sequestered within the CD1a cleft, where it is fully inaccessible to TCRs. Most known amphipathic membrane lipids, such as sulfatide or SM (*19*), occupy nearly all of the CD1a cleft and then extend their head groups through a portal (F′ portal) onto the external surface of CD1a (Fig. 5C). In contrast, farnesol occupies only 36% of the cleft. Accordingly, this relatively small ligand could have been seated in many ways within the larger cavity or potentially bound with lipid:CD1 stoichiometry of 2:1 or 3:1 (*52*). Instead, a preferred seating and orientation of a single molecule is observed at the junction of the A′ and F′ pockets. Unlike CD1b structures in which two lipids bind simultaneously within the cleft (*53*, *54*), electron density corresponding to a second lipid or spacer in the cleft was not observed (Fig. 5, A and B). This finding agreed with elution experiments showing substantial exclusion of the measured self-lipids from CD1a complexes (Fig. 4E). Together, the biochemical and structural data indicated that farnesol itself was sufficient to stabilize a partially occupied CD1a cleft.

Farnesol is buried fully within CD1a

In previously solved CD1a structures in complex with oleic acid (*35*) or an acyl peptide (*40*), the flexible fatty acyl chains take a C-shaped conformation around the margin of the curved A′ pocket (Fig. 5D) (*19*, *35*, *40*). These lipids encircle a vertical structure known as the A′ pole, which is formed by an interaction of Phe^{70} and Val^{12}, located in the ceiling and floor of the A′ pocket, respectively (Fig. 5B, inset) (*19*, *35*, *40*). The semi-rigid and branched structure of farnesol does not allow the C-shaped peripheral conformation seen with other lipids and instead lies in the center of the A′ pocket, disrupting the A′ pole. The orientation of farnesol is discernible: The terminal methyl and hydroxyl groups point toward the A′ and F′ pocket, respectively (Fig. 5B). The polar hydroxyl group is situated nearer the solvent-exposed F′ portal of CD1a with ~15% of its surface water exposed. Farnesol made van der Waals contacts with Phe^{10}, Trp^{14}, Phe^{70}, Val^{98}, Leu^{161}, Leu^{162}, and Phe^{169} from CD1a (Fig. 5B and table S2). Here, Trp^{14} stacked against the unsaturated hydrocarbons C12 and C14 of farnesol, further stabilizing the bound lipid within the cleft. The same Trp^{14} residue maintains hydrophobic contacts with sphingosine and acyl chain moieties in the CD1a-SM and CD1a-sulfatide structures (*19*), respectively. Collectively, this positioning mechanism appears to be driven by unsaturations in farnesol, which limit its ability to bend and provide van der Waals interactions with the inner surface of CD1a.

Parallels in the positioning of CD1a-urushiol and CD1a-farnesol (Fig. 5E) highlight how the positioning of bulky and constrained lipids differs from the seating of acyl chain–containing ligands (Fig. 5D). Although farnesol and urushiol are not located in the same position, they are both situated near the junction of the A′ and F′ pockets (Fig. 5E) and do not take the deep and curved positioning at the rim of the A′ toroid (Fig. 5D). Whereas oleate and acyl peptide wrap around the intact A′ pole [Fig. 5B (inset) and D], farnesol and urushiol complexes show a marked repositioning of Phe^{70}, which disrupts the A′ pole (Fig. 5, B and E). Urushiol extends substantially into the F′-pocket so that it approaches the F′ portal of CD1a. It is unknown whether TCRs contact urushiol, but the molecule is adjacent to the surface portal (*30*), and TCRs can contact lipids located just within the portal (*55*). In contrast, farnesol is ~8 Å more deeply positioned, so that it is unequivocally separated from the F′ portal and the TCR contact surface (Fig. 5E).

Overall, the structure-activity relationships (Fig. 3) indicated that many small, hydrophobic, bulky lipids from consumer goods are recognized by T cells. The biochemical (Fig. 4) and structural (Fig. 5) analyses of CD1a-lipid complexes demonstrate that farnesol's small size and unsaturated structure allow it to interact specifically, but not covalently, within CD1a. This binding interaction stabilizes the CD1a cleft and positions farnesol out of the reach of the TCR, largely or fully displacing lipids that normally emerge to the outer surface of CD1a (*19*, *35*, *40*).

DISCUSSION

In 1963, Gell and Coombs (*3*) classified human disease–related immune manifestations into four types of hypersensitivity reactions. Despite the early development and descriptive nature of this scheme, the classification system is still widely taught in clinical immunology and medicine. Type I, II, and III reactions are rapid and mediated by B cells, whereas the delayed type IV response is mediated by T cells. Our study sought molecular mechanisms underpinning type IV hypersensitivity to the most common contact dermatitis allergens in consumer products. Our data provide specific molecular connections between CD1a-reactive T cells and four structurally related contact dermatitis allergens: benzyl benzoate, benzyl cinnamate, farnesol, and coenzyme Q–related compounds. Whereas haptens (*9*), drugs (*7*), or cations (*8*) can influence MHC-peptide display, here, we detail a straightforward mechanism for T cell activation by small molecules that noncovalently bind CD1a.

In the MHC and CD1 systems, the most common recognition mechanism involves TCR cocontact with an epitope on the carried peptide or lipid and the antigen-presenting molecule (*21*, *56*–*58*). Here, we show evidence that the key active components of balsam of Peru and farnesol activate T cells by binding to CD1a without cellular processing. However, both the structural and biochemical data strongly point to a new model of recognition that does not involve TCR contact with epitopes present on the stimulatory small molecules. Antigenic tree oils, PPBF, farnesol, coenzyme Q2, and the other 14 oily stimulants identified here all lack carbohydrate, phosphate, or peptidic groups that normally serve as TCR epitopes. We show that the BC2 TCR can cross-react among at least 16 stimulatory compounds, which do not share any single chemical structure that would be a candidate cross-reactive epitope. More conclusively, farnesol resides deeply within the CD1a cleft, essentially ruling out direct contact with the TCR. Sequestration of molecules of a small size could be a general mechanism of their recognition, because all of the stimulatory molecules are smaller than the CD1a cleft (*21*, *40*, *57*).

Prior studies of CD1-lipid complexes have emphasized head group positioning, where the seating of amphipathic lipids in the cleft is guided by carbohydrates or charged moieties that interact near the F′ portal. Alkyl chains have a "bland" repetitive structure and have been described as sliding within CD1 allowing diversely positioning in the groove (*54*, *59*). On the basis of this concept, we expected that the small hydrophobic ligands studied here might slide freely or adopt multiple positions in the CD1a cleft. Also, because many of the lipids have a molecular size that is less than half the volume of the CD1a cleft, they might have bound in pairs or together with spacer lipids (*52*, *53*, *60*, *61*). However, farnesol shows one defined position in the CD1a groove. Both MS and crystallographic analysis failed to detect cobinding spacer lipids, indicating that partial occupancy by one small lipid is sufficient to stabilize the CD1a cleft.

Comparison of CD1a-farnesol with previously solved CD1a-lipid structures provides insight into the roles of steric hindrance and interior pocket remodeling. CD1a-oleate (*35*), CD1a–mycobactin-like lipopeptide (*40*), CD1a-sulfatide (*19*), and CD1a-SM (*35*) complexes involve lipids with flexible alkyl chains. These alkyl chains insert deeply into CD1a by curling along the outer wall of the A′ pocket and wrapping around the A′ pole to insert fully within the cleft (*40*). In contrast, farnesol is chemically hindered and bulky, on the basis of polyunsaturation and methyl branching. The rigid and bulky moiety in urushiol derives from a substituted catechol ring. These two molecules cannot curl to trace the outer wall of the A′ pocket and so do not penetrate deeply, and both sit in a central position within the A′ pocket that prevents the A′ pole from forming. Farnesol is anchored in a specific position by a series of van der Waals interactions with named pocket residues formed by its polyunsaturated and branched structure. Although the roles of benzyl rings in benzyl benzoate and benzyl cinnamate are not studied structurally, they also constrain the chemical structure in ways that are also expected to prevent the side wall curvature (*19*, *35*, *40*). More generally, many of the stimulatory lipids identified here and in a recent study (*31*)—including farnesol, squalene, geranylgeraniol, geranylgeranylacetone, and coenzyme Q2—are polyunsaturated or branched isoprenoid lipids that could plausibly anchor in CD1a by similar mechanisms.

Lipid antigen binding wholly within CD1a could trigger T cell responses by remodeling the three-dimensional structure of CD1a, as previously reported for CD1d (*62*, *63*), CD1b (*54*), and CD1c (*41*, *64*). However, comparing CD1a-farnesol with all CD1a-lipid structures solved to date (*19*, *35*, *40*) does not demonstrate a broad or obvious change in CD1a conformation. Also, binding of the BC2 TCR to both CD1a-farnesol and CD1a-endo points away from this explanation. Instead, biochemical analysis of CD1a-endo complexes and the CD1a-farnesol structure both indicate that farnesol displaces endogenous ligands from the cleft. Whereas farnesol can be considered a headless ligand, some amphipathic self-lipid ligands in CD1a-endo structures have head groups composed of phosphates or sugars that normally cover the exposed surface of CD1a (*35*). In the case of the SM, it blocks autoreactive T cells by interfering with TCR contact with CD1a (*31*, *35*). Our experimental observations rule in key aspects of the absence of interference model, where activating substances are sequestered within the CD1a cleft, so that recognition occurs by ejecting self-lipids and freeing up epitopes on the surface of CD1a itself.

As contrasted with MHC I and MHC II, where peptides are broadly exposed over the lateral dimension of the platform, human CD1 proteins have a large roof-like structure above their clefts and a small antigen exit portal at the margin of the platform (*65*). This creates a potentially large, ligand-free TCR contact surface on CD1 proteins. Evidence for the predominant contact of αβ TCRs with the surface of CD1 proteins in preference to carried lipids, including the extreme case in which TCRs contact CD1 only, is becoming a central theme in CD1 research (*65*). Recent studies have shown direct TCR contact with the unliganded surface of CD1a and CD1c by autoreactive clones and polyclonal T cells (*31*, *35*, *42*). Thus, the stimulatory compounds identified here, which are small and internally sequestered, provide a molecular link to polyclonal autoreactive T cell responses, which are specific for the surface of CD1 rather than the carried lipid.

The presence of CD1a in all individuals prompts the question of why allergic contact dermatitis does not universally develop in everyone. However, interindividual differences that may play a role include permeability of the skin barrier (*66*), dose and number of chemical exposures to allergens, regulatory T cell activity (*67*–*69*), and interindividual differences in T cell repertoires. Prior studies show that there is interindividual variability in the frequency of CD1a-restricted T cells in the blood and skin of healthy individuals and differences in CD1a-autoreactive response rates in skin (*25*, *66*, *70*, *71*). Increased CD1a-restricted T cells responses were observed in allergic individuals and those with inflammatory skin disease (*66*, *70*, *72*), which

may be a factor in susceptibility to development of CD1a-mediated allergic contact dermatitis in certain individuals. Consistent with these known patterns of antigen response, our small study of 11 humans demonstrates differing patterns of polyclonal response in each individual rather than a universal response to one antigen, which might be expected from an innate receptor.

Overall, the molecular analysis of tree oils and isoprenoid lipids presented in this manuscript invites focused consideration of the role of CD1a in T cell–mediated skin diseases. In this new view, the pattern of high-density CD1a on the Langerhans cell network present throughout the skin could mediate responses to oils naturally produced within the skin or oils that contact the skin through application of commercial skin products containing botanical extracts, synthetic lipids, or oils. Other immunogenic oils used in human patients or for experimental biology include the adjuvant MF-59 (squalene) and incomplete Freund's adjuvant (mineral oil). These immunogens, as well as drug-like small molecules resembling PPBF or sulfonamide antibiotics, could plausibly act through the CD1 system.

MATERIALS AND METHODS

Study design

The goal of this study was to determine whether known contact allergens can bind to CD1a and stimulate a CD1a-dependent T cell response. This study involved in vitro T cell assays using both CD1a-restricted T cell lines and polyclonal purified T cells from healthy blood bank donors. For T cell recognition, either cell-based assays using CD1a-expressing APCs or CD1a plate assays using recombinant plate-bound CD1a were performed. Cytokine release was measured by ELISA, and/or cytokine transcription was measured by real-time qPCR. Complex lipid mixtures, such as balsam of Peru, were purified by TLC and analyzed by nanoelectrospray ionization MS. Lipid eluents from CD1a, after displacement by contact allergens, were analyzed by positive normal-phase HPLC-quadrupole time-of-flight (QToF)–MS. Structural insights into CD1a complexed with the contact allergen farnesol were obtained by x-ray crystallography.

Contact dermatitis antigen screen

T.R.U.E. Test panel 1 (Truetest 1) is a patch test routinely used in clinic to diagnose contact dermatitis in response to the most common allergens (SmartPractice, Phoenix, AZ). The system consists of surgical tape (5.2 cm by 13.0 cm) that is embedded with antigen patches of 0.81 cm^2 with each coated with a polyester film that contains uniformly dispersed specific allergen. Using sterile technique, individual allergen patches were cut and placed directly in the assay wells containing ~10^6 APCs and 1 ml of T cell media in 24-well plates (contact method) or first extracted by soaking patch in 1 ml of media (2 hours, 37°C), followed by removing the patch and transferring 100 μl of media to T cell assays. Antigen dose was normalized to square millimeters of patch exposure. Antigens or extracts were cocultured with 50,000 CD1a- or mock-transfected K562 cells (*25*) and a CD1a-dependent T cell line in a 96-well plate. Activation was measured by IFN-γ ELISA (Thermo Fisher Scientific).

CD1a assays for T cell antigens

Balsam of Peru, balsam of Peru oil, benzyl cinnamate, and benzyl benzoate or other isolated antigens were dried in clean glass, subjected to water bath sonication in T cell media for 120 s, cultured with 50,000 CD1a- or mock-transfected K562 cells for 3 hours at 37°C, and then cocultured with 50,000 to 200,000 cells per well of an autoreactive T cell line (BC2 or Bgp) (*31*) or foreign antigen reactive T cells (CD8-2) (*18*) for 24 hours at 37°C in 96-well plates as previously described (*31*). Activation was measured using IFN-γ ELISA (Thermo Fisher Scientific). For blocking experiments, CD1a-transfected K562 cells were preincubated for 1 hour at 37°C with CD1a-blocking antibody (OKT-6) or isotype-matched control immunoglobulin G (P3) (10 μg/ml) before the addition of T cells. For plate assays, 96-well streptavidin plates (Thermo Fisher Scientific) were incubated for 24 hours at room temperature with biotinylated CD1a or CD1b protein [10 μg/ml; National Institutes of Health (NIH) Tetramer Core Facility] and anti-CD11a (2.5 μg/ml) in phosphate-buffered saline (PBS) (pH 7.4) as previously described (*31*). For the acid-stripping protocol (Figs. 4 and 5A and fig. S2), after 24 hours of coating with protein, plates were washed three times with PBS, followed by washing twice with citrate buffer at pH 3.4 for 10 min, followed by three washes in PBS before the addition of lipid antigens (*30*). Peripheral blood mononuclear cells (PBMC) were isolated from buffycoats obtained from the New York Blood Center, as approved by the Institutional Review Board of Columbia University Irving Medical Center. Polyclonal T cell assays were performed using FACS (fluorescence-activated cell sorting)–sorted T cells from PBMCs ($CD4^-$ and $CD4^+$) and CD1a-coated 96-well plates as described above. Plate-coated CD1a was either treated with buffer only (0.05% CHAPS in PBS) or lipid antigens sonicated in buffer and incubated overnight at 37°C. Plates were washed three times, and then purified T cells were added to the wells and incubated overnight at 37°C. RNA was extracted using RNeasy (Qiagen), and first-strand complementary DNA synthesis was performed using iScript (Bio-Rad).

Lipid sources

Balsam of Peru (W211613), balsam of Peru oil (W211710), benzyl cinnamate (234214), benzyl benzoate (B9550), geranylgeraniol (G3278), farnesol (277541), geranylgeranyl acetone (G5048), geraniol (163333), squalene (S3626), geranyl acetone (250716), vitamin K1 (V3501), vitamin K2 (V9378), vitamin A (R7632), vitamin E (T3251), vitamin D3 (C9756), coenzyme Q2 (C8081), coenzyme Q0 (D9150), coenzyme Q4 (C2470), coenzyme Q6 (C9504), coenzyme Q10 (C9538), palmitoleic acid (P9417), methyl palmitoleate (P9667), *cis*-11-hexadecenal (249084), palmityl acetate (P0260), palmitoleyl alcohol (P1547), lauryl palmitoleate (P1642), oleamide (O2136), palmitoyl ethanolamide (P0359), tetradecanoic acid ethylamide (R425567), *N*-oleoyl glycin (O9762), *N*,*N*-dimethyl tetradecanamide (S347388), and 1-dodecyl-2-pyrrolidinone (335673) were obtained from Sigma-Aldrich (St. Louis, MO). Coenzyme Q1 (270-294-M002) was obtained from Alexis Biochemicals.

Lipid analysis by TLC

Silica-coated glass TLC plates (10 cm by 20 cm; Scientific Adsorbents Incorporated) were precleared in chloroform-methanol-water (60:30:6, v/v/v). Samples (10 to 20 μg) were developed with a solvent system-hexane/diethyl ether/acetic acid (70/30/1, v/v/v). For visualization, plates were sprayed with a solution of 3% (w/v) of cupric acetate in 8% (v/v) phosphoric acid, followed by heating for 20 to 30 min at 150°C.

Nanoelectrospray ionization MS

Methanol solution (2 μg/ml) was prepared for each reagent, and then, 10 μl was loaded onto a glass nanospray tip for positive-mode electrospray ionization MS performed on an LXQ (Thermo Scientific),

two-dimensional ion trap mass spectrometer. The spray voltage and capillary temperature were set to 0.8 kV and 200°C.

High-performance liquid chromatography–QToF–MS

CD1a-endo (200 μg) and CD1a-farnesol (200 μg) were transferred to 15-ml glass tubes and treated with chloroform, methanol, and water for lipid extraction according to the method of Bligh and Dyer (*73*). The lipid-containing organic solvent layer was separated from the top aqueous layer by centrifugation at 850*g* for 10 min. For HPLC-MS analysis, the samples were normalized on the basis of the input proteins (20 μM), and 20 μl of eluent was injected to an Agilent 6530 Accurate-Mass Q-TOF spectrometer equipped with a 1260 series HPLC system using a normal-phase Inertsil diol column (150 mm by 2.1 mm, 3 μm; GL Sciences) with a guard column (10 mm by 3 mm, 3 μm; GL Sciences), running at 0.15 ml/min according to a published method (*74*).

Recombinant CD1a expression and purification

The glycoprotein CD1a was expressed in human embryonic kidney (HEK) 293S GnTI$^-$ cells and purified as previously described (*35*). After an endoglycosidase H (New England BioLabs) and thrombin treatment, the purified CD1a was first loaded with the ganglioside GD_3 (GD_3) (Avanti) that was dissolved in a solution containing 2.5% dimethyl sulfoxide (DMSO) and 0.5% tyloxapol (Sigma-Aldrich). CD1a was first incubated overnight with GD_3 at room temperature at a molar ratio of 1:8. The CD1a sample loaded with GD_3 was further purified using ion exchange chromatography (MonoQ 10/100 GL, GE Healthcare). *Trans*,*trans*-farnesol (Sigma-Aldrich) was dissolved in a solution containing 2.5% DMSO and 0.5% tyloxapol (Sigma-Aldrich). The CD1a-GD_3 sample was then incubated overnight with farnesol at a 1:100 molar ratio and at room temperature. A subsequent ion exchange chromatography (MonoQ 10/100 GL) was performed to remove the excess of farnesol, CD1a-GD_3, and tyloxapol.

Expression, refolding, and purification of recombinant TCRs

The BC2 TCR was produced using a previously described method (*31*). Briefly, individual α and β chains of the TCR, with an engineered disulfide bond between the TCRα and TCRβ constant domains were expressed in BL21 *Escherichia coli* cells as inclusion bodies and solubilized in 8 M urea buffer containing 10 mM tris-HCl (pH 8), 0.5 mM Na-EDTA, and 1 mM dithiothreitol. The TCR was then refolded in buffer that was composed of 5 M urea, 100 mM tris-HCl (pH 8), 2 mM Na-EDTA, 400 mM L-Arg-HCl, 0.5 mM oxidized glutathione, and 5 mM reduced glutathione. The refolded solution was dialyzed twice against 10 mM tris-HCl (pH 8.0) overnight. The dialyzed samples were then purified through DEAE cellulose, size exclusion, and anion exchange HiTrap Q chromatography approaches. The quality and purity of the samples were analyzed via SDS–polyacrylamide gel electrophoresis.

Crystallization, structure determination, and refinement

Seeds obtained from previous binary CD1a antigen crystals (*30*) were used to grow crystals of the CD1a-farnesol binary complex in 20 to 25% polyethylene glycol 1500/10% DL-Malic acid, MES monohydrate, Tris (MMT) buffer (pH 5 to 6). The crystals were flash-frozen, and data were collected at the MX2 beamline (Australian Synchrotron) to a resolution of 2.2 Å. All the data were processed with the program XDS (*75*) and were scaled with SCALA from the CCP4 programs suite (*76*). Upon successful phasing by molecular replacement using the program PHASER (*77*) and the CD1a-urushiol structure as the search model (*30*), the farnesol electron density was evident in the unbiased electron density maps in addition to some very weak residual density. An initial run of rigid body refinement was performed using phenix.refine (*78*). Iterative model improvement was performed using with the program COOT (*79*) and phenix.refine. The final refinement led to an R/R-free (%) of 20/25. The quality of the structure was confirmed at the Research Collaboratory for Structural Bioinformatics Protein Data Bank Data Validation and Deposition Services website. All presentations of molecular graphics were created with UCSF Chimera (*80*).

Surface plasmon resonance

Biotinylated CD1a-endogenous lipids derived from HEK293 cells was incubated overnight with 30-fold molar excess of farnesol solubilized in 2.5% DMSO/0.5% tyloxapol (CD1a-farnesol) or with solvent only (CD1a-mock). The sample was coupled onto research-grade streptavidin-coated chips to a mass concentration of ~3000 resonance units. Increasing concentrations of the BC2 TCR (0 to 200 μM) were injected over all flow cells for 30 s at a rate of 5 μl/min on a Biacore 3000 in 10 mM tris-HCl (pH 8) and 150 mM NaCl buffer. The final response was calculated by subtraction of the response for CD1a-endogenous minus a flow cell containing an unrelated protein. The data were fitted to a 1:1 Langmuir binding model using BIAevaluation version 3.1 software (Biacore AB) and the equilibrium data analyzed using Prism program for biostatistics, curve fitting, and scientific graphing (GraphPad).

Statistical analyses

All statistical analyses were performed in R (www.R-project.org/). Pairwise *t* tests, analysis of variance (ANOVA) post hoc testing, and adjustments of *P* values for multiple hypothesis testing used base R and the package emmeans (https://CRAN.R-project.org/package=emmeans). Dose-response analyses used the package drc to fit log normal or logistic curves to the data and to test fitted models against simplified, pooled models (*81*). R code is available on request.

SUPPLEMENTARY MATERIALS

immunology.sciencemag.org/cgi/content/full/5/43/eaax5430/DC1

Fig. S1. Screening human T cells for responses to known contact allergens.
Fig. S2. CD1a-dependent T cell response to small hydrophobic molecules.
Fig. S3. Idebenone is recognized by CD1a-restricted T cell line BC2.
Fig. S4. CD1a-dependent polyclonal T cell responses to contact allergens.
Fig. S5. CD1a tetramer staining of CD1a-autoreactive T cell line.
Fig. S6. Electron density for farnesol in CD1a-farnesol binary complex.
Table S1. Supporting data CD1a-farnesol binary complex.
Table S2. Van der Waals bonds between CD1a and farnesol.
Table S3. Raw data sets for main figures (Excel spreadsheet).

View/request a protocol for this paper from *Bio-protocol*.

REFERENCES AND NOTES

1. M. Peiser, T. Tralau, J. Heidler, A. M. Api, J. H. Arts, D. A. Basketter, J. English, T. L. Diepgen, R. C. Fuhlbrigge, A. A. Gaspari, J. D. Johansen, A. T. Karlberg, I. Kimber, J. P. Lepoittevin, M. Liebsch, H. I. Maibach, S. F. Martin, H. F. Merk, T. Platzek, T. Rustemeyer, A. Schnuch, R. J. Vandebriel, I. R. White, A. Luch, Allergic contact dermatitis: Epidemiology, molecular mechanisms, in vitro methods and regulatory aspects. Current knowledge assembled at an international workshop at BfR, Germany. *Cell Mol. Life Sci.* **69**, 763–781 (2012).
2. D. H. Kaplan, B. Z. Igyártó, A. A. Gaspari, Early immune events in the induction of allergic contact dermatitis. *Nat. Rev. Immunol.* **12**, 114–124 (2012).

3. P. G. H. Gell, R. R. A. Coombs, *Clinical Aspects of Immunology* (Blackwell, Oxford, 1963), vol. 1.
4. D. N. Garboczi, P. Ghosh, U. Utz, Q. R. Fan, W. E. Biddison, D. C. Wiley, Structure of the complex between human T-cell receptor, viral peptide and HLA-A2. *Nature* **384**, 134–141 (1996).
5. K. C. Garcia, M. Degano, R. L. Stanfield, A. Brunmark, M. R. Jackson, P. A. Peterson, L. Teyton, I. A. Wilson, An αβ T cell receptor structure at 2.5 Å and its orientation in the TCR-MHC complex. *Science* **274**, 209–219 (1996).
6. J. Rossjohn, S. Gras, J. J. Miles, S. J. Turner, D. I. Godfrey, J. McCluskey, T cell antigen receptor recognition of antigen-presenting molecules. *Annu. Rev. Immunol.* **33**, 169–200 (2015).
7. P. T. Illing, J. P. Vivian, N. L. Dudek, L. Kostenko, Z. Chen, M. Bharadwaj, J. J. Miles, L. Kjer-Nielsen, S. Gras, N. A. Williamson, S. R. Burrows, A. W. Purcell, J. Rossjohn, J. McCluskey, Immune self-reactivity triggered by drug-modified HLA-peptide repertoire. *Nature* **486**, 554–558 (2012).
8. G. M. Clayton, Y. Wang, F. Crawford, A. Novikov, B. T. Wimberly, J. S. Kieft, M. T. Falta, N. A. Bowerman, P. Marrack, A. P. Fontenot, S. Dai, J. W. Kappler, Structural basis of chronic beryllium disease: Linking allergic hypersensitivity and autoimmunity. *Cell* **158**, 132–142 (2014).
9. K. Landsteiner, J. Jacobs, Studies on the sensitization of animals with simple chemical compounds. II. *J. Exp. Med.* **64**, 625–639 (1936).
10. M. Schmidt, B. Raghavan, V. Müller, T. Vogl, G. Fejer, S. Tchaptchet, S. Keck, C. Kalis, P. J. Nielsen, C. Galanos, J. Roth, A. Skerra, S. F. Martin, M. A. Freudenberg, M. Goebeler, Crucial role for human Toll-like receptor 4 in the development of contact allergy to nickel. *Nat. Immunol.* **11**, 814–819 (2010).
11. C. Burkhart, M. Britschgi, I. Strasser, J. P. Depta, S. von Greyerz, V. Barnaba, W. J. Pichler, Non-covalent presentation of sulfamethoxazole to human $CD4^+$ T cells is independent of distinct human leucocyte antigen-bound peptides. *Clin. Exp. Allergy* **32**, 1635–1643 (2002).
12. J. Farrell, M. Lichtenfels, A. Sullivan, E. C. Elliott, A. Alfirevic, A. V. Stachulski, M. Pirmohamed, D. J. Naisbitt, B. K. Park, Activation of carbamazepine-responsive T-cell clones with metabolically inert halogenated derivatives. *J. Allergy Clin. Immunol.* **132**, 493–495 (2013).
13. S. Sieben, Y. Kawakubo, T. Al Masaoudi, H. F. Merk, B. Blömeke, Delayed-type hypersensitivity reaction to paraphenylenediamine is mediated by 2 different pathways of antigen recognition by specific $\alpha\beta^+$ human T-cell clones. *J. Allergy Clin. Immunol.* **109**, 1005–1011 (2002).
14. M. Keller, M. Lerch, M. Britschgi, V. Tâche, B. O. Gerber, M. Lüthi, P. Lochmatter, G. Kanny, A. J. Bircher, C. Christiansen, W. J. Pichler, Processing-dependent and -independent pathways for recognition of iodinated contrast media by specific human T cells. *Clin. Exp. Allergy* **40**, 257–268 (2010).
15. J. Adam, W. J. Pichler, D. Yerly, Delayed drug hypersensitivity: Models of T-cell stimulation. *Br. J. Clin. Pharmacol.* **71**, 701–707 (2011).
16. B. B. Levine, Z. Ovary, Studies on the mechanism of the formation of the penicillin antigen. III. The N-(D-α-benzylpenicilloyl) group as an antigenic determinant responsible for hypersensitivity to penicillin G. *J. Exp. Med.* **114**, 875–940 (1961).
17. M. Bharadwaj, P. Illing, A. Theodossis, A. W. Purcell, J. Rossjohn, J. McCluskey, Drug hypersensitivity and human leukocyte antigens of the major histocompatibility complex. *Annu. Rev. Pharmacol. Toxicol.* **52**, 401–431 (2012).
18. D. B. Moody, D. C. Young, T.-Y. Cheng, J.-P. Rosat, C. Roura-Mir, P. B. O'Connor, D. M. Zajonc, A. Walz, M. J. Miller, S. B. Levery, I. A. Wilson, C. E. Costello, M. B. Brenner, T cell activation by lipopeptide antigens. *Science* **303**, 527–531 (2004).
19. D. M. Zajonc, M. A. Elsliger, L. Teyton, I. A. Wilson, Crystal structure of CD1a in complex with a sulfatide self antigen at a resolution of 2.15 Å. *Nat. Immunol.* **4**, 808–815 (2003).
20. Z.-H. Zeng, A. R. Castaño, B. W. Segelke, E. A. Stura, P. A. Peterson, I. A. Wilson, Crystal structure of mouse CD1: An MHC-like fold with a large hydrophobic binding groove. *Science* **277**, 339–345 (1997).
21. M. Salio, J. D. Silk, E. Y. Jones, V. Cerundolo, Biology of CD1- and MR1-restricted T cells. *Annu. Rev. Immunol.* **32**, 323–366 (2014).
22. I. Van Rhijn, D. C. Young, J. S. Im, S. B. Levery, P. A. Illarionov, G. S. Besra, S. A. Porcelli, J. Gumperz, T.-Y. Cheng, D. B. Moody, CD1d-restricted T cell activation by nonlipidic small molecules. *Proc. Natl. Acad. Sci. U.S.A.* **101**, 13578–13583 (2004).
23. R. J. Betts, A. Perkovic, S. Mahapatra, A. Del Bufalo, K. Camara, A. R. Howell, S. Martinozzi Teissier, G. De Libero, L. Mori, Contact sensitizers trigger human CD1-autoreactive T-cell responses. *Eur. J. Immunol.* **47**, 1171–1180 (2017).
24. S. K. Dougan, A. Kaser, R. S. Blumberg, CD1 expression on antigen-presenting cells. *Curr. Top. Microbiol. Immunol.* **314**, 113–141 (2007).
25. A. de Jong, V. Peña-Cruz, T.-Y. Cheng, R. A. Clark, I. Van Rhijn, D. B. Moody, CD1a-autoreactive T cells are a normal component of the human αβ T cell repertoire. *Nat. Immunol.* **11**, 1102–1109 (2010).
26. C. de Lalla, M. Lepore, F. M. Piccolo, A. Rinaldi, A. Scelfo, C. Garavaglia, L. Mori, G. De Libero, P. Dellabona, G. Casorati, High-frequency and adaptive-like dynamics of human CD1 self-reactive T cells. *Eur. J. Immunol.* **41**, 602–610 (2011).
27. M. Sugita, E. P. Grant, E. van Donselaar, V. W. Hsu, R. A. Rogers, P. J. Peters, M. B. Brenner, Separate pathways for antigen presentation by CD1 molecules. *Immunity* **11**, 743–752 (1999).
28. V. Manolova, M. Kistowska, S. Paoletti, G. M. Baltariu, H. Bausinger, D. Hanau, L. Mori, G. De Libero, Functional CD1a is stabilized by exogenous lipids. *Eur. J. Immunol.* **36**, 1083–1092 (2006).
29. C. Kobayashi, T. Shiina, A. Tokioka, Y. Hattori, T. Komori, M. Kobayashi-Miura, T. Takizawa, K. Takahara, K. Inaba, H. Inoko, M. Takeya, G. Dranoff, M. Sugita, GM-CSF-independent CD1a expression in epidermal Langerhans cells: Evidence from human CD1A genome-transgenic mice. *J. Invest. Dermatol.* **132**, 241–244 (2012).
30. J. H. Kim, Y. Hu, T. Yongqing, J. Kim, V. A. Hughes, J. Le Nours, E. A. Marquez, A. W. Purcell, Q. Wan, M. Sugita, J. Rossjohn, F. Winau, CD1a on Langerhans cells controls inflammatory skin disease. *Nat. Immunol.* **17**, 1159–1166 (2016).
31. A. de Jong, T.-Y. Cheng, S. Huang, S. Gras, R. W. Birkinshaw, A. G. Kasmar, I. Van Rhijn, V. Peña-Cruz, D. T. Ruan, J. D. Altman, J. Rossjohn, D. B. Moody, CD1a-autoreactive T cells recognize natural skin oils that function as headless antigens. *Nat. Immunol.* **15**, 177–185 (2014).
32. A. F. Fransway, K. A. Zug, D. V. Belsito, V. A. Deleo, J. F. Fowler Jr., H. I. Maibach, J. G. Marks, C. G. Mathias, M. D. Pratt, R. L. Rietschel, D. Sasseville, F. J. Storrs, J. S. Taylor, E. M. Warshaw, J. Dekoven, M. Zirwas, North American contact dermatitis group patch test results for 2007–2008. *Dermatitis* **24**, 10–21 (2013).
33. R. Wolf, E. Orion, E. Ruocco, A. Baroni, V. Ruocco, Contact dermatitis: Facts and controversies. *Clin. Dermatol.* **31**, 467–478 (2013).
34. M. Swamy, K. Beck-Garcia, E. Beck-Garcia, F. A. Hartl, A. Morath, O. S. Yousefi, E. P. Dopfer, E. Molnár, A. K. Schulze, R. Blanco, A. Borroto, N. Martín-Blanco, B. Alarcon, T. Höfer, S. Minguet, W. W. Schamel, A cholesterol-based allostery model of T cell receptor phosphorylation. *Immunity* **44**, 1091–1101 (2016).
35. R. W. Birkinshaw, D. G. Pellicci, T.-Y. Cheng, A. N. Keller, M. Sandoval-Romero, S. Gras, A. de Jong, A. P. Uldrich, D. B. Moody, D. I. Godfrey, J. Rossjohn, αβ T cell antigen receptor recognition of CD1a presenting self lipid ligands. *Nat. Immunol.* **16**, 258–266 (2015).
36. J.-P. Rosat, E. P. Grant, E. M. Beckman, C. C. Dascher, P. A. Sieling, D. Frederique, R. L. Modlin, S. A. Porcelli, S. T. Furlong, M. B. Brenner, CD1-restricted microbial lipid antigen-specific recognition found in the $CD8^+$ αβ T cell pool. *J. Immunol.* **162**, 366–371 (1999).
37. T. Hamilton, G. C. de Gannes, Allergic contact dermatitis to preservatives and fragrances in cosmetics. *Skin Therapy Lett.* **16**, 1–4 (2011).
38. D. C. Young, D. B. Moody, T-cell recognition of glycolipids presented by CD1 proteins. *Glycobiology* **16**, 103R–112R (2006).
39. D. B. Moody, D. M. Zajonc, I. A. Wilson, Anatomy of CD1–lipid antigen complexes. *Nat. Rev. Immunol.* **5**, 387–399 (2005).
40. D. M. Zajonc, M. D. Crispin, T. A. Bowden, D. C. Young, T.-Y. Cheng, J. Hu, C. E. Costello, P. M. Rudd, R. A. Dwek, M. J. Miller, M. B. Brenner, D. B. Moody, I. A. Wilson, Molecular mechanism of lipopeptide presentation by CD1a. *Immunity* **22**, 209–219 (2005).
41. S. Mansour, A. S. Tocheva, C. Cave-Ayland, M. M. Machelett, B. Sander, N. M. Lissin, P. E. Molloy, M. S. Baird, G. Stübs, N. W. Schröder, R. R. Schumann, J. Rademann, A. D. Postle, B. K. Jakobsen, B. G. Marshall, R. Gosain, P. T. Elkington, T. Elliott, C.-K. Skylaris, J. W. Essex, I. Tews, S. D. Gadola, Cholesteryl esters stabilize human CD1c conformations for recognition by self-reactive T cells. *Proc. Natl. Acad. Sci. U.S.A.* **113**, E1266–E1275 (2016).
42. K. S. Wun, J. F. Reijneveld, T.-Y. Cheng, K. Ladell, A. P. Uldrich, J. Le Nours, K. L. Miners, J. E. McLaren, E. J. Grant, O. L. Haigh, T. S. Watkins, S. Suliman, S. Iwany, J. Jimenez, R. Calderon, K. L. Tamara, S. R. Leon, M. B. Murray, J. A. Mayfield, J. D. Altman, A. W. Purcell, J. J. Miles, D. I. Godfrey, S. Gras, D. A. Price, I. Van Rhijn, D. B. Moody, J. Rossjohn, T cell autoreactivity directed toward CD1c itself rather than toward carried self lipids. *Nat. Immunol.* **19**, 397–406 (2018).
43. T. Kawano, J. Cui, Y. Koezuka, I. Toura, Y. Kaneko, K. Motoki, H. Ueno, R. Nakagawa, H. Sato, E. Kondo, H. Koseki, M. Taniguchi, CD1d-restricted and TCR-mediated activation of $v_\alpha 14$ NKT cells by glycosylceramides. *Science* **278**, 1626–1629 (1997).
44. D. B. Moody, B. B. Reinhold, M. R. Guy, E. M. Beckman, D. E. Frederique, S. T. Furlong, S. Ye, V. N. Reinhold, P. A. Sieling, R. L. Modlin, G. S. Besra, S. A. Porcelli, Structural requirements for glycolipid antigen recognition by CD1b-restricted T cells. *Science* **278**, 283–286 (1997).
45. A. Schnuch, W. Uter, J. Geier, H. Lessmann, P. J. Frosch, Contact allergy to farnesol in 2021 consecutively patch tested patients. Results of the IVDK. *Contact Dermatitis* **50**, 117–121 (2004).
46. M. A. Mc Aleer, P. Collins, Allergic contact dermatitis to hydroxydecyl ubiquinone (idebenone) following application of anti-ageing cosmetic cream. *Contact Dermatitis* **59**, 178–179 (2008).
47. J. Natkunarajah, L. Ostlere, Allergic contact dermatitis to idebenone in an over-the-counter anti-ageing cream. *Contact Dermatitis* **58**, 239 (2008).
48. D. Sasseville, L. Moreau, M. Al-Sowaidi, Allergic contact dermatitis to idebenone used as an antioxidant in an anti-wrinkle cream. *Contact Dermatitis* **56**, 117–118 (2007).
49. D. Zhou, J. Mattner, C. Cantu III, N. Schrantz, N. Yin, Y. Gao, Y. Sagiv, K. Hudspeth, Y.-P. Wu, T. Yamashita, S. Teneberg, D. Wang, R. L. Proia, S. B. Levery, P. B. Savage, L. Teyton, A. Bendelac, Lysosomal glycosphingolipid recognition by NKT cells. *Science* **306**, 1786–1789 (2004).
50. M. Kronenberg, W. L. Havran, Immunology: Oiling the wheels of autoimmunity. *Nature* **506**, 42–43 (2014).

51. A. J. Corbett, S. B. Eckle, R. W. Birkinshaw, L. Liu, O. Patel, J. Mahony, Z. Chen, R. Reantragoon, B. Meehan, H. Cao, N. A. Williamson, R. A. Strugnell, D. Van Sinderen, J. Y. Mak, D. P. Fairlie, L. Kjer-Nielsen, J. Rossjohn, J. McCluskey, T-cell activation by transitory neo-antigens derived from distinct microbial pathways. *Nature* **509**, 361–365 (2014).
52. S. Huang, T.-Y. Cheng, D. C. Young, E. Layre, C. A. Madigan, J. Shires, V. Cerundolo, J. D. Altman, D. B. Moody, Discovery of deoxyceramides and diacylglycerols as CD1b scaffold lipids among diverse groove-blocking lipids of the human CD1 system. *Proc. Natl. Acad. Sci. U.S.A.* **108**, 19335–19340 (2011).
53. S. D. Gadola, N. R. Zaccai, K. Harlos, D. Shepherd, J. C. Castro-Palomino, G. Ritter, R. R. Schmidt, E. Y. Jones, V. Cerundolo, Structure of human CD1b with bound ligands at 2.3 Å, a maze for alkyl chains. *Nat. Immunol.* **3**, 721–726 (2002).
54. L. F. Garcia-Alles, A. Collmann, C. Versluis, B. Lindner, J. Guiard, L. Maveyraud, E. Huc, J. S. Im, S. Sansano, T. Brando, S. Julien, J. Prandi, M. Gilleron, S. A. Porcelli, H. de la Salle, A. J. Heck, L. Mori, G. Puzo, L. Mourey, G. De Libero, Structural reorganization of the antigen-binding groove of human CD1b for presentation of mycobacterial sulfoglycolipids. *Proc. Natl. Acad. Sci. U.S.A.* **108**, 17755–17760 (2011).
55. S. Gras, I. Van Rhijn, A. Shahine, T.-Y. Cheng, M. Bhati, L. L. Tan, H. Halim, K. D. Tuttle, L. Gapin, J. Le Nours, D. B. Moody, J. Rossjohn, T cell receptor recognition of CD1b presenting a mycobacterial glycolipid. *Nat. Commun.* **7**, 13257 (2016).
56. D. M. Zajonc, The CD1 family: Serving lipid antigens to T cells since the Mesozoic era. *Immunogenetics* **68**, 561–576 (2016).
57. N. A. Borg, K. S. Wun, L. Kjer-Nielsen, M. C. Wilce, D. G. Pellicci, R. Koh, G. S. Besra, M. Bharadwaj, D. I. Godfrey, J. McCluskey, J. Rossjohn, CD1d–lipid-antigen recognition by the semi-invariant NKT T-cell receptor. *Nature* **448**, 44–49 (2007).
58. K. C. Garcia, M. Degano, L. R. Pease, M. Huang, P. A. Peterson, L. Teyton, I. A. Wilson, Structural basis of plasticity in T cell receptor recognition of a self peptide-MHC antigen. *Science* **279**, 1166–1172 (1998).
59. D. B. Moody, How T cells grasp mycobacterial lipid antigens. *Proc. Natl. Acad. Sci. U.S.A.* **114**, 13312–13314 (2017).
60. L. F. Garcia-Alles, K. Versluis, L. Maveyraud, A. T. Vallina, S. Sansano, N. F. Bello, H. J. Gober, V. Guillet, H. de la Salle, G. Puzo, L. Mori, A. J. Heck, G. De Libero, L. Mourey, Endogenous phosphatidylcholine and a long spacer ligand stabilize the lipid-binding groove of CD1b. *EMBO J.* **25**, 3684–3692 (2006).
61. R. N. Cotton, A. Shahine, J. Rossjohn, D. B. Moody, Lipids hide or step aside for CD1-autoreactive T cell receptors. *Curr. Opin. Immunol.* **52**, 93–99 (2018).
62. C. McCarthy, D. Shepherd, S. Fleire, V. S. Stronge, M. Koch, P. A. Illarionov, G. Bossi, M. Salio, G. Denkberg, F. Reddington, A. Tarlton, B. G. Reddy, R. R. Schmidt, Y. Reiter, G. M. Griffiths, P. A. van der Merwe, G. S. Besra, E. Y. Jones, F. D. Batista, V. Cerundolo, The length of lipids bound to human CD1d molecules modulates the affinity of NKT cell TCR and the threshold of NKT cell activation. *J. Exp. Med.* **204**, 1131–1144 (2007).
63. K. S. Wun, G. Cameron, O. Patel, S. S. Pang, D. G. Pellicci, L. C. Sullivan, S. Keshipeddy, M. H. Young, A. P. Uldrich, M. S. Thakur, S. K. Richardson, A. R. Howell, P. A. Illarionov, A. G. Brooks, G. S. Besra, J. McCluskey, L. Gapin, S. A. Porcelli, D. I. Godfrey, J. Rossjohn, A molecular basis for the exquisite CD1d-restricted antigen specificity and functional responses of natural killer T cells. *Immunity* **34**, 327–339 (2011).
64. L. Scharf, N.-S. Li, A. J. Hawk, D. Garzón, T. Zhang, L. M. Fox, A. R. Kazen, S. Shah, E. J. Haddadian, J. E. Gumperz, A. Saghatelian, J. D. Faraldo-Gómez, S. C. Meredith, J. A. Piccirilli, E. J. Adams, The 2.5 Å structure of CD1c in complex with a mycobacterial lipid reveals an open groove ideally suited for diverse antigen presentation. *Immunity* **33**, 853–862 (2010).
65. I. Van Rhijn, D. I. Godfrey, J. Rossjohn, D. B. Moody, Lipid and small-molecule display by CD1 and MR1. *Nat. Rev. Immunol.* **15**, 643–654 (2015).
66. R. Jarrett, M. Salio, A. Lloyd-Lavery, S. Subramaniam, E. Bourgeois, C. Archer, K. L. Cheung, C. Hardman, D. Chandler, M. Salimi, D. Gutowska-Owsiak, J. B. de la Serna, P. G. Fallon, H. Jolin, A. McKenzie, A. Dziembowski, E. I. Podobas, W. Bal, D. Johnson, D. B. Moody, V. Cerundolo, G. Ogg, Filaggrin inhibits generation of CD1a neolipid antigens by house dust mite–derived phospholipase. *Sci. Transl. Med.* **8**, 325ra318 (2016).
67. U. Luckey, T. Schmidt, N. Pfender, M. Romer, N. Lorenz, S. F. Martin, T. Bopp, E. Schmitt, A. Nikolaev, N. Yogev, A. Waisman, T. Jakob, K. Steinbrink, Crosstalk of regulatory T cells and tolerogenic dendritic cells prevents contact allergy in subjects with low zone tolerance. *J. Allergy Clin. Immunol.* **130**, 781–797.e11 (2012).
68. A. Braun, N. Dewert, F. Brunnert, V. Schnabel, J.-H. Hardenberg, B. Richter, K. Zachmann, S. Cording, A. Claßen, R. Brans, A. Hamann, J. Huehn, M. P. Schön, Integrin α_E (CD103) is involved in regulatory T-cell function in allergic contact hypersensitivity. *J. Invest. Dermatol.* **135**, 2982–2991 (2015).
69. A. El Beidaq, C. W. Link, K. Hofmann, B. Frehse, K. Hartmann, K. Bieber, S. F. Martin, R. J. Ludwig, R. A. Manz, In vivo expansion of endogenous regulatory T cell populations induces long-term suppression of contact hypersensitivity. *J. Immunol.* **197**, 1567–1576 (2016).
70. S. Subramaniam, A. Aslam, S. A. Misbah, M. Salio, V. Cerundolo, D. B. Moody, G. Ogg, Elevated and cross-responsive CD1a-reactive T cells in bee and wasp venom allergic individuals. *Eur. J. Immunol.* **46**, 242–252 (2016).
71. C. S. Hardman, Y.-L. Chen, M. Salimi, R. Jarrett, D. Johnson, V. J. Järvinen, R. J. Owens, E. Repapi, D. J. Cousins, J. L. Barlow, A. N. J. McKenzie, G. Ogg, CD1a presentation of endogenous antigens by group 2 innate lymphoid cells. *Sci. Immunol.* **2**, eaan5918 (2017).
72. K. L. Cheung, R. Jarrett, S. Subramaniam, M. Salimi, D. Gutowska-Owsiak, Y. L. Chen, C. Hardman, L. Xue, V. Cerundolo, G. Ogg, Psoriatic T cells recognize neolipid antigens generated by mast cell phospholipase delivered by exosomes and presented by CD1a. *J. Exp. Med.* **213**, 2399–2412 (2016).
73. E. G. Bligh, W. J. Dyer, A rapid method of total lipid extraction and purification. *Can. J. Biochem. Physiol.* **37**, 911–917 (1959).
74. E. Layre, L. Sweet, S. Hong, C. A. Madigan, D. Desjardins, D. C. Young, T.-Y. Cheng, J. W. Annand, K. Kim, I. C. Shamputa, M. J. McConnell, C. A. Debono, S. M. Behar, A. J. Minnaard, M. Murray, C. E. Barry III, I. Matsunaga, D. B. Moody, A comparative lipidomics platform for chemotaxonomic analysis of Mycobacterium tuberculosis. *Chem. Biol.* **18**, 1537–1549 (2011).
75. W. Kabsch, Xds. *Acta Crystallogr. D Biol. Crystallogr.* **66**, 125–132 (2010).
76. M. D. Winn, C. C. Ballard, K. D. Cowtan, E. J. Dodson, P. Emsley, P. R. Evans, R. M. Keegan, E. B. Krissinel, A. G. Leslie, A. McCoy, S. J. McNicholas, G. N. Murshudov, N. S. Pannu, E. A. Potterton, H. R. Powell, R. J. Read, A. Vagin, K. S. Wilson, Overview of the CCP4 suite and current developments. *Acta Crystallogr. D Biol. Crystallogr.* **67**, 235–242 (2011).
77. A. J. McCoy, R. W. Grosse-Kunstleve, P. D. Adams, M. D. Winn, L. C. Storoni, R. J. Read, Phaser crystallographic software. *J. Appl. Cryst.* **40**, 658–674 (2007).
78. P. V. Afonine, R. W. Grosse-Kunstleve, N. Echols, J. J. Headd, N. W. Moriarty, M. Mustyakimov, T. C. Terwilliger, A. Urzhumtsev, P. H. Zwart, P. D. Adams, Towards automated crystallographic structure refinement with phenix.refine. *Acta Crystallogr. D Biol. Crystallogr.* **68**, 352–367 (2012).
79. P. Emsley, B. Lohkamp, W. G. Scott, K. Cowtan, Features and development of Coot. *Acta Crystallogr. D Biol. Crystallogr.* **66**, 486–501 (2010).
80. E. F. Pettersen, T. D. Goddard, C. C. Huang, G. S. Couch, D. M. Greenblatt, E. C. Meng, T. E. Ferrin, UCSF chimera—A visualization system for exploratory research and analysis. *J. Comput. Chem.* **25**, 1605–1612 (2004).
81. C. Ritz, F. Baty, J. C. Streibig, D. Gerhard, Dose-response analysis using R. *PLOS ONE* **10**, e0146021 (2015).

Acknowledgments: We thank A. G. Kasmar, M. C. Castells, and P. Brennan for advice or critical comments on the manuscript. We thank the staff at the Australian Synchrotron for assistance with data collection and the NIH Tetramer Core Facility for recombinant biotinylated CD1 protein. **Funding:** S.N. was supported by an NIH training grant (T32 AI007306) and is currently employed by HealthPartners, St. Paul, Minnesota. A.d.J. is supported by a K01 award from the NIH (K01 AR068475) and an Irving Scholarship from the Irving Institute for Clinical and Translational Research at Columbia University. D.B.M. is supported by the NIH (R01 AR048632) and the Wellcome Trust Collaborative Award. This work was supported by the National Health and Medical Research Council of Australia (NHMRC) and the Australian Research Council (ARC) (CE140100011). J.L.N. is supported by an ARC Future Fellowship (FT160100074); J.R. is supported by an Australian ARC Laureate Fellowship and the Wellcome Trust Collaborative Award. Research reported in this publication was performed in the CCTI Flow Cytometry Core, supported, in part, by the Office of the Director, NIH under award S10OD020056. **Author contributions:** The indicated individuals carried out project oversight and direction (A.d.J., D.B.M., and J.R.); T cell assays (S.N., T.-Y.C., E.A.B., R.N.C., I.V.R., G.C.M., and A.d.J.); protein chemistry, structure, and SPR (M.W. and J.L.N.); and manuscript preparation (S.N., A.d.J., D.B.M., and J.R.) with input from all authors. **Competing interests:** The authors declare that they have no competing interests. **Data and materials availability:** Reagents are available to qualified scientists subject to the limitation that cells from primary T cell lines can be limited in number. The data and refined coordinates for the CD1a-farnesol structure were deposited in the Protein Data Bank under accession code 6NUX. All other data needed to evaluate the conclusions in the paper are present in the paper or the Supplementary Materials.

Submitted 3 April 2019
Accepted 5 December 2019
Published 3 January 2020
10.1126/sciimmunol.aax5430

Citation: S. Nicolai, M. Wegrecki, T.-Y. Cheng, E. A. Bourgeois, R. N. Cotton, J. A. Mayfield, G. C. Monnot, J. Le Nours, I. Van Rhijn, J. Rossjohn, D. B. Moody, A. de Jong, Human T cell response to CD1a and contact dermatitis allergens in botanical extracts and commercial skin care products. *Sci. Immunol.* **5**, eaax5430 (2020).

Science Immunology

Human T cell response to CD1a and contact dermatitis allergens in botanical extracts and commercial skin care products

Sarah Nicolai, Marcin Wegrecki, Tan-Yun Cheng, Elvire A. Bourgeois, Rachel N. Cotton, Jacob A. Mayfield, Gwennaëlle C. Monnot, Jérôme Le Nours, Ildiko Van Rhijn, Jamie Rossjohn, D. Branch Moody and Annemieke de Jong

Sci. Immunol. **5**, eaax5430.
DOI: 10.1126/sciimmunol.aax5430

Oily skin allergens hole up inside CD1a

Contact dermatitis induced by allergens in personal care products is a common cause of skin rashes, but the molecular mechanisms leading to T cell activation are poorly understood. Nicolai *et al.* tested known contact allergens for their ability to boost IFN-γ production by human T cells autoreactive to the CD1a antigen presentation molecule. Several hydrophobic chemicals came up as "hits," including farnesol, a compound often used as a fragrance. Structural analysis of CD1a-farnesol complexes revealed that farnesol is buried deep within CD1a's antigen-binding cleft beyond the reach of T cell receptor chains. These findings suggest that several hydrophobic contact allergens elicit T cell–mediated hypersensitivity reactions through displacement of self-lipids normally bound to CD1a, thereby exposing T cell–stimulatory surface regions of CD1a that are normally hidden.